Design and optimization method for 3D printed carbon reinforced aircraft components

Authors: W.M. van den Brink[1], F. van der Klift[2], R. Bruins[1], M.J.M. Hermans[2]

[1] Netherlands Aerospace Centre (NLR), The Netherlands
[2] Delft University of Technology, The Netherlands

Keywords: Composite structures, Aerospace, 3D printing, Finite elements

ABSTRACT

Recent developments in the field of plastic additive manufacturing have seen the introduction of carbon fibres in printed products. These fibres improve the strength and stiffness of the thermoplastic based components. Two approaches are currently seen, the very short fibre embedded in the printing filament and continuous fibres, where the focus for this research is on the latter. The improvements observed to strength and stiffness from adding continuous fibres are very interesting and could be used to optimize parts and reduce weight, which is important for aerospace applications, see Figure 1. However the design approaches currently use trial and error to determine the fibre content in the parts. A design and analyses method is proposed to predict the mechanical behaviour of the material and the printed components with parameters such as fibre type, geometry and filling.

The novel method proposed for the continuous fibre reinforced 3D printed design uses the finite element approach. The thermoplastic and the fibre are meshed independently and are combined using numerical algorithms. From the independent meshes the local element stiffness response is calculated and the stress, strain and deformation of the components can be predicted. The approach is very flexible; the fibre mesh can be adjusted independently so that the local reinforcement design can be changed and optimized. The mechanical properties of the fibres, thermoplastic material and layer adhesion are calibrated using test data on coupon level.

Figure 1: On the left the Airbus A350 for which main components are constructed from carbon fibre reinforced material (source: Airbus). On the right 3D printed examples reinforced with carbon fibres in the contour (source: MarkForged)

The proposed method can further be used to predict manufacturing induced effects which are mainly related to temperature changes. Thermoplastic material tends to shrink when cooled down, which

combined with the layered approach in 3D printing causes large residual stresses. These stresses may cause distortion of the component or even failure during the printing process. The proposed method is capable to predict these thermal effects. With the presented approach, 3D printing with continuous carbon fibres is moving from the current trial and error approach to right first time designs. This enables further optimization of the component design and process parameters, achieving weight reduction. The application of this technology in aerospace non-critical components, if more mature, is foreseen for interior parts such as hinges or seat frames.

1 INTRODUCTION

Over the last decades the NLR has developed experience in the field of high performance composite structures for aerospace components. The manufacturing methods have moved over the years from mainly hand lay-up to automated systems using the Fibre Placement Manufacturing (FPM) [2]. Furthermore, in view of optimizing the composite component performance, there has been extensive research done on fibre steering methods. In previous research it has been shown that the performance of fibre steered design can outperform the classical composite lay-up designs [1].

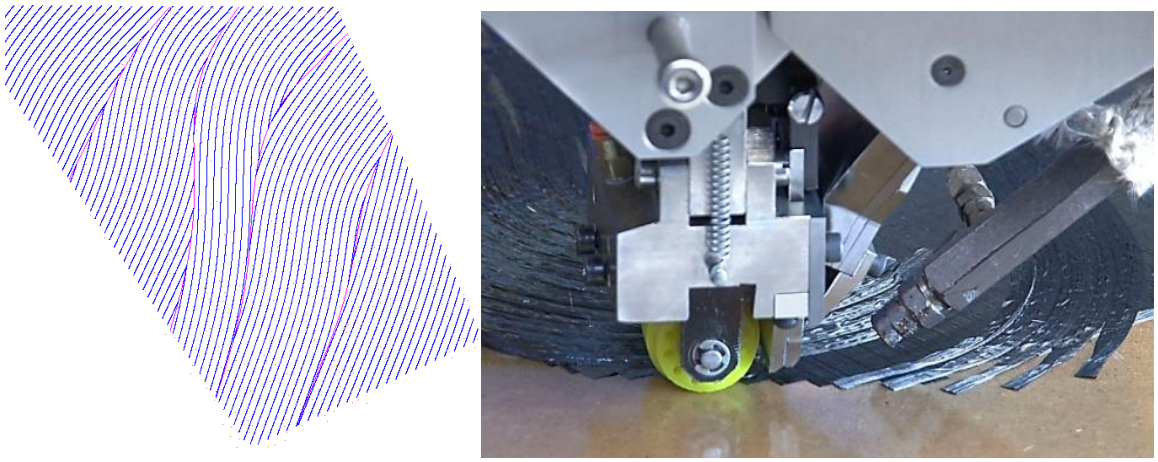

Figure 2: On the left the fibre steered design for a business jet horizontal stabilizer investigated in the TAPAS2 project [1], [2]. On the right the use of fibre steering on the composite fibre placement machine at NLR

Additive manufacturing (AM) has had a large impact on industry and society in the recent years in the fields of e.g. design, prototyping, healthcare [4, 5] and military purposes [6]. Reasons for this are the ability to create almost any complex shape [7] and the possible reduction of production costs [9, 10]. Harris [11] reported that nearly 90% of all AM machines sold, were 3D printers for polymer based parts. In 2011, Berman [8] found that in 2011 desktop 3D printers were already available for 10.000 USD a piece. Nowadays, everyone can buy their own 3D printer starter kit for prices around 300 Euro and build themselves a basic polymer hobby 3D printer.

The main problem with the 3D printing of polymer materials is the mechanical properties of the parts, especially for structural applications [12]. Adding fibres to the polymer increases the mechanical properties, however, not all AM techniques are capable of achieving this [13], see Figure 3. Ning[14] reported that FDM (Fused Deposition Modelling) and SLS (Selective Laser Sintering) processes have been adapted to fabricate fibre reinforced plastics. These fibres can be chopped or continuous fibres, where the chopped fibres have inferior mechanical properties compared to continuous fibres for unidirectional performance [15]. Tekinalp et al. [16] compared the FDM printing CFRP (Continuous

Fibre Reinforced Plastics) with compress moulding CFRP and came to the conclusion that the FDM technique creates parts with a higher void area. Results from Namiki et al.[17] and van der Klift et al.[18] showed that there were significant void area formations for 3D printing composites with continuous fibres via the FDM technique.

Matsuzaki et al.[19] created continuous fibre reinforced composites via in-nozzle impregnation and showed that this is also possible for jute fibre composites, which are easier to recycle. However, higher strengths are needed for aerospace structural applications, which already has been achieved by Love et al.[20]

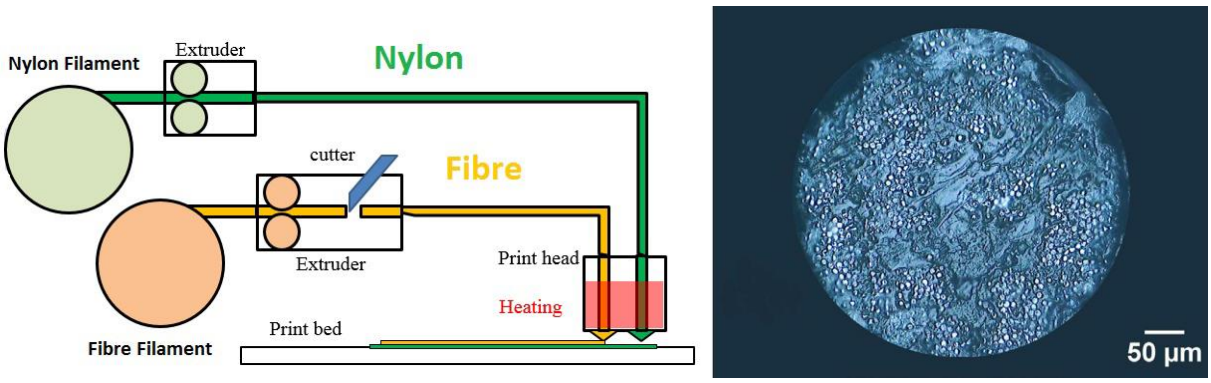

Figure 3: Schematic of the MarkTwo® 3D printer using a nylon base filament and continuous fibre filled filament. These are combined on the print bed. On the right a cross section of the carbon fibre filled filament where the low fibre volume fraction of 34.5% can be observed.

It has to be stated that all of the results above have been obtained through trial and error, which can be a very costly way of obtaining results, especially for the carbon fibre reinforced materials. In this paper the authors look to generate predictive models of unidirectional carbon fibre reinforced nylon material with the MarkTwo 3D printer, of which the previous version has been described by van der Klift et al. Since this printer is the only commercial available this is used as the baseline for this method.

The typical layer thickness and properties for the printer are:

- Nylon layer: 0.125 mm
- Filled fibre layer: 0.125 mm
- Wall thickness is 0.4 mm
- Typical offset per fibre path: 0.4 mm

The performance and applicability of the CFRP 3D printer will be compared with the current manufacturing methods used. For the numerical evaluation of the 3D printed designs an independent mesh method will be used to capture the effects of the carbon fibres in the printed component. The knowledge in the field of high performance composite design including fibre steering optimization and manufacturing is used in this research for application on 3D printed parts. The introduction of finite element methods for fibre reinforced 3D printed plastic components is a novel field of research.

2 METHOD

The research performed resulted in an independent mesh meso-macro composite model created to investigate the effect of local fibre volume fraction variation in the 3D printed composites. This allows

for improvements and evaluation of the performance of the design under load, also called virtual testing. The micro-level experimental data performed in this project is used to define ‘yarn’ dimension and mechanical properties. The macro experiments are used for model calibration and validation. Within the meso-macro model the yarns are geometrically modelled with beam elements using a Python script to mimic the real design, see Figure 4. With the fibre designs in the nylon base material with the corresponding fibre directions, curvature and local stiffness variation is achieved.[3]

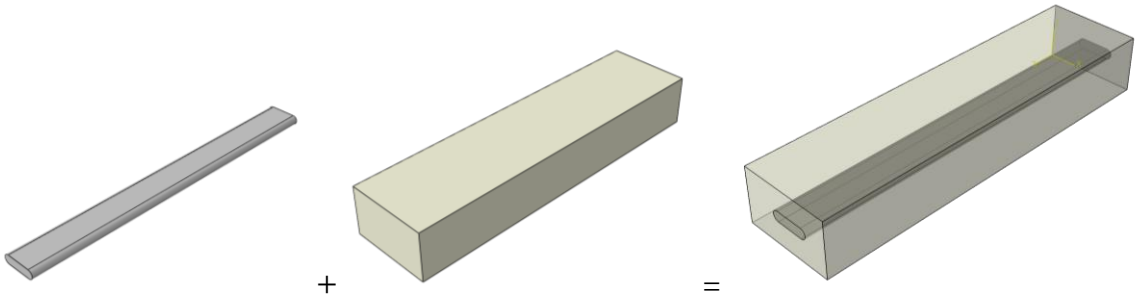

Figure 4: Overview of adding the carbon fibre geometric representation on the left to the nylon ‘host’ material in the middle. The result is a combined material using independent meshes.

The individual yarns are ‘bonded’ with the volumetric matrix geometry using the embedded element method within Abaqus. This enables the use of independent meshes to be combined and thus representing the 3D printed composite, as shown in Figure 5. From the models topology the distance between nodes of the embedded elements (carbon fibres) and the host element (nylon) is calculated. If an embedded node lies within a host element at a certain distance, the translational degrees of freedom of the embedded node are interpolated from the host element using a constraint. Consequently this constraint can introduce additional spurious stiffness and may lead to wrong results. This will be investigated with the calibration and validation cases. The stiffness contributions from the nylon host elements and the fibres are included separately in the model. Here for, it is assumed that the local carbon fibre support material in the filament is also nylon.

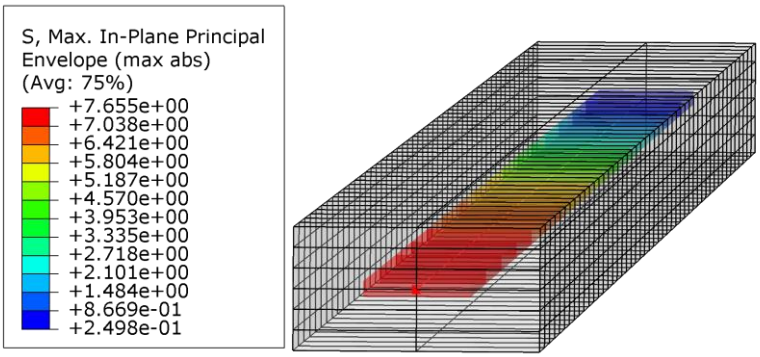

Figure 5: Mesh independent numerical model for a carbon fibre reinforced 3D printed example on one fibre. The loads are indicative. The coloured lines indicate the stress in the carbon fibres modelled as beam elements with a tension load in fibre direction.

The material properties for the nylon material and the carbon fibre are derived from test results on tension and bending coupons. The properties are calibrated in the numerical model to capture the coupon stiffness and strength behaviour. This calibrated material data is then later used on component design level.

The first step in the numerical approach is to map the design from the Eiger tool inside the Abaqus software to allow for finite element calculations. Since there is no exporting option in the Eiger software for the defined fibre path a separate python tool is created to extract the paths. This python tool is based on the outer contour of the sliced section of geometry. Then an offset is defined from this outer contour to design the layers in the part. This approach is very similar to the one that Eiger uses, although simplified. The results of this method and approach are shown in the next section. Also the experimental result on the tensile and bending tests performed is shown.

The carbon fibre reinforced 3D printing process provides more design freedom than that is possible with the currently available printers. Two main design aspects can be optimized to increase the component mechanical performance and therefore the design approach for 3D print components can be divided in two steps:

1. The polymer contour geometry can be adjusted to allow for load effective load transfer.
2. The design of the carbon fibres in the polymer base can be optimized for maximum performance or low weight.

In the first step the baseline design is used in a topology optimization to enable optimal load paths and reduction in weight. This topology optimization is commercial available and relative mature. For this the Abaqus Tosca tools are used. Usually there is significant rework needed on the optimized design to make it printable and reduced stress concentrations. The second step would be to optimize the carbon fibre paths in the 3D print. This second step is strongly limited by the web-based slicer (Eiger) of the MarkTwo printer which does not allow for customized fibre designs. In the approach the slicer limits are investigated and if needed further steps will be taken, meaning that the design cannot be manufactured as desired. Further development in the field of 3D printers using continuous fibres is anticipated.

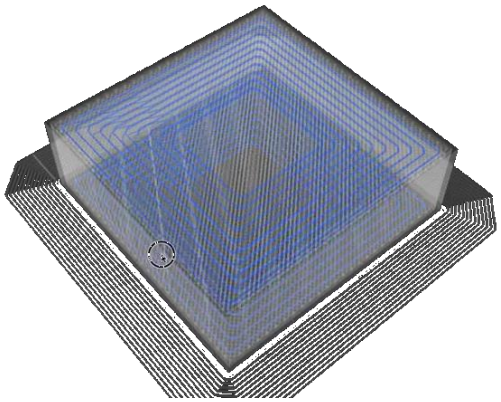

Figure 6: Example from the web-based Eiger tool to design the fibre paths per layer (in blue)

3 RESULTS

For the evaluation of the material stiffness, strength and microstructure, several samples are printed and tested. In a previous research by one of the authors, the theoretical performance of a tensile test sample with six out or ten layers reinforced with carbon fibres, has a relatively high performance compared to standard construction materials as is seen in table 1.

Table 1- values from van der Klift et al.[15] comparing the MarkForged material (6CF 18%) with common construction materials. The AS4/8552 is a typical high performance carbon epoxy composite material.

Material Name	*Tensile Strength [MPa]*	*Tensile Modulus [GPa]*	*Density [g/cm^3]*	*Specific Strength [kN·m/kg]*	*Specific Stiffness [kN·m/kg]*
SS400	400	206	7.9	50.6	26100
S45C	690	205	7.8	88.5	26300
A2017P	355	69	2.8	127	24600
A2024P	430	74	2.8	154	26400
Ti-6Al-4V	980	106	4.4	223	24100
AS4/8552 UD CFRP	2230	141	1.58	1411	89240
60%CF (Toray®)	1860	135	1.6	**1160**	**84400**
6CF 18% CF[15]	464.4	35.7	1.42	**327**	**25140**

In order to create a valid model, several mechanical properties have to be known. The most important ones being the tensile strength, tensile modulus, flexural strength, flexural modulus, compressive strength and finally the compressive modulus. For determining these properties, three types of samples were created. The first one is a tensile test specimen and will be tested in accordance to ASTM D3039-14.[21] The second type of specimen is a flexural 3-point bending test specimen according to the rules of the ASTM D790–03[22]. The third type is a compressive specimen which is designed according to EN2850 [23].

It was chosen to create the samples in such a way that all three types of coupons could be obtained from a single print. In total 5 samples were printed, which were sawed into 15 coupons, 5 tensile coupons, 5 bending coupons, and 5 compression coupons. Fig. 2.1 shows the sample once printed by the MarkTwo.

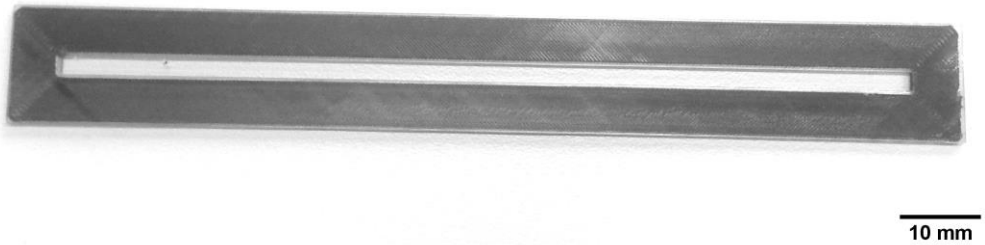

Figure 7: Picture of the printed samples from which the tensile, bending and compression coupons are extracted. The thickness is 2 mm.

It was chosen to not use tabs on the tensile test coupons, due to a rather large amount of nylon surrounding the fibres, which should be sufficient to prevent any clamping damage to the fibre material. The hydraulic pressure, however, was halved in order to not crush the coupons, and was equal to 1000 psi. The test temperature was 23.0° C with a relative humidity of 50 %.

The raw data obtained from the tensile tests was used to draw stress-strain graphs on the results. The stress-strain graph resulting from this data can be seen in Figure 8. It should be noted that all coupons have been tested until final failure occurred.

The T1, T2 and T3 had the LAB failure mode, while coupon T4 and T5 failed in LAT. These failure modes are explained in the ASTM D3039-14 [21]. LAB means the sample failed lateral at the bottom grip. LAT means a lateral failure occurred at the top grip.

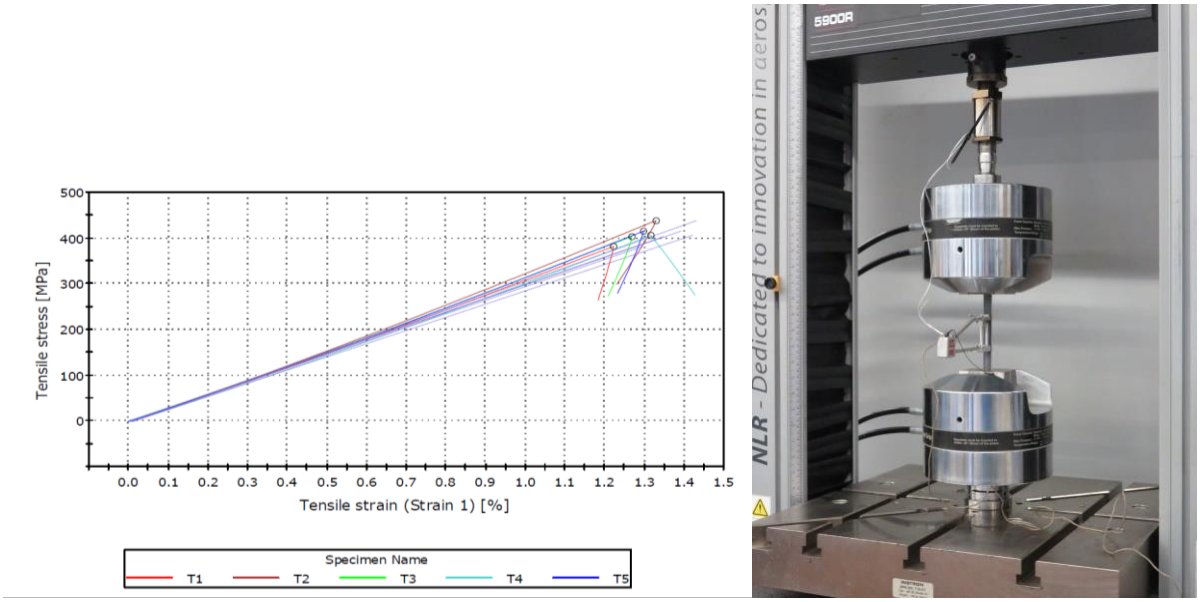

Figure 8: Results of the tensile tests for five coupons and test setup on the right

It can be concluded that the scatter of the results is relatively low, even though there is a relatively large dimensional inaccuracy with a 2.44 % variation in the thickness. The coefficient of variation in table 3.1 shows that the ultimate tensile stress has a scatter of at maximum 5 % whereas the Young's modulus only has a scatter of less than 2.5 %.

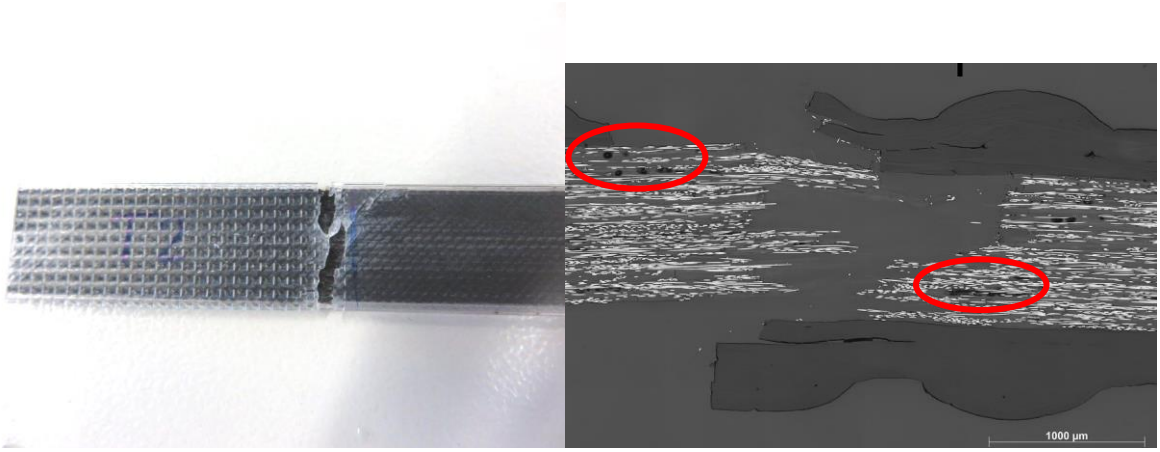

Figure 9: Failure mode of the tensile T2 coupon and micro structure cross section view of the failure mode. The nylon floor and top layers can be identified. Also significant void areas are observed in this cross section indicated in red.

The bending tests and the compression test were also conducted. An interesting result to discuss is the amount of energy stored in the tensile test coupons during testing, which is common for the D3039

tests. This energy was sufficient enough to, once the coupon failed, cause partial compressive failure on the other end of the sample. The stored energy, once released, make the coupon jump back to its original size so fast that at least the nylon layers locally delaminated from the CFRP core of the coupon. From the experiments the mechanical properties of the composite were defined to be used for the finite element calculations.

Table 2; Material properties from experimental data

Material Name	*Tensile Strength [MPa]*	*Tensile Modulus [GPa]*	*Flexural Strength [MPa]*	*Flexural Modulus [GPa]*	*Fibre fill percentage [%]*
Coupon test results	409	29.8	144	7.16	14.15
Nylon	50-90	0.50			0.0
Fibre yarn	1032	71.11			34.5

The mechanical properties resulting from the tests performed at the NLR show that the strength and stiffness increase compared to typical 3D print plastic e.g. nylon, PLA, ABS is significant. This makes the material interesting to use in low or medium loaded parts in an aircraft. For example brackets in the interior or seat-frames which are currently made of aluminium. A weight gain can be achieved in theory although more research is needed. The reinforcement is in one or multiple layers in a 2D plane where the strength perpendicular to these layers (z-direction of the print) is of the nylon base material. The strength of the nylon base material is lower than from the carbon fibre, see Table 2. Hence typical applications are where the load is transferred in a 2D plane. It has to be noted that quality issues with the current process need to be addressed, in particular the void and adhesion issues observed through the microscope.

From the test results a translation is made to the mechanical properties of the carbon fibre yarn to be used in the calculations. Here the stiffness of the nylon is neglected. From this it can be concluded that the maximum load per carbon fibre yarn is 113.4 [N] and combined for the total coupon this results in the tension failure load of 12.1 kN on average. The tension and bending coupon is simulated using finite element and the method is described in section 2, see Figure 10.

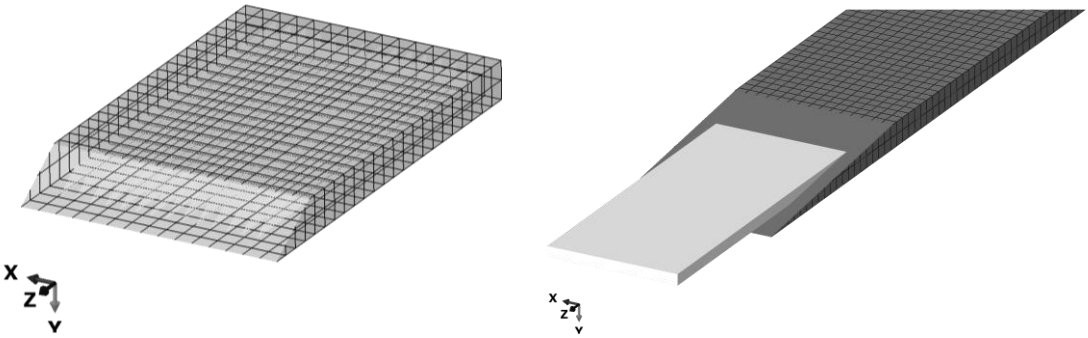

Figure 10: Finite element model of the coupon geometry with the nylon host geometry and the 112 individual carbon yarns

The main purpose of the coupon model is to evaluate the independent mesh approach and to verify whether the tensile and bending stiffness values are correct using the same mechanical properties. Also the effect of the load introduction on the local strain and stress is evaluated. From the simulation it

shows that overall the stress is uniform however there is a higher stress observed near the support region. Also the large stiffness difference between the carbon fibre yarns and the nylon can lead to hour glassing in the elements, see Figure 11.

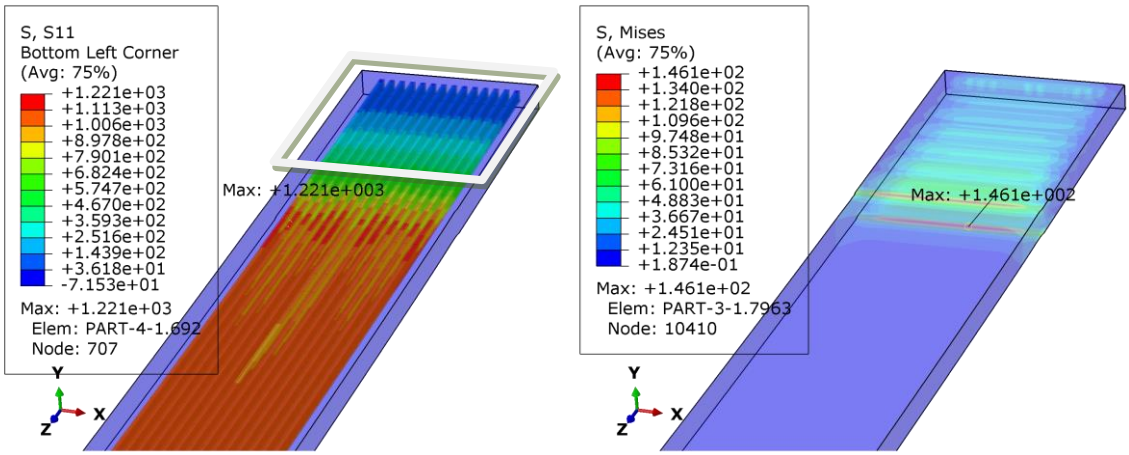

Figure 11: On the left the stress in the carbon fibre yarns with the support region indicated and on the right only the nylon host stress values. At some point in the nylon plasticity will occur which is not included in this simulation

From the simulation significant shearing of the outer nylon layers is observed caused by the relatively low stiffness. Interestingly the local highest stress of 1221 MPa is higher than the average stress of 1032 from the global maximum force of the coupon. Hence there are test effects which result in a lower maximum stress for the material. The simulation of the bending setup is performed in a similar manner, only with a non-linear solver because of the large deflection. The load is applied as pressure on a small region in the centre of the coupon. The coupon is supported on two rollers with an offset of 100 mm as in the experiment, see Figure 12.

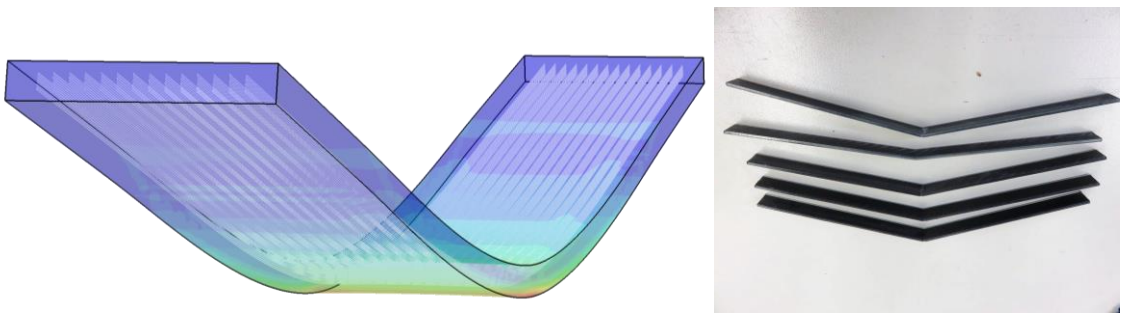

Figure 12: bending simulation using the independent mesh approach showing the strain. On the bottom there is a tensile strain as expected. On the right the failure bending coupons

The results of the bending simulations show a very similar behaviour using the data from the tension experiments. Although this is not a perfect validation, it gives an indication whether the material properties and the independent meshing method used is valid. The same nonlinear effect can be observed in both the test and simulation and the final maximum displacement is similar.

Outlook

Using the data obtained from the experiments in combination with the analyses method presented in this paper allows for numerical evaluation of the 3D printed designs. A simple 2D example is taken of

a bracket connecting two load points and with a hole inside. A topology optimization has been performed to define the geometry outline. This is followed by a fibre steering optimization approach to find the optimum performance. This in turn is translated to fibre paths which can be placed using the 3D print continuous fibre technology. This is a first step into the optimization and will be developed further in the future. This section is merely to show the workflow and does not show the optimal design .The starting geometry is a simple bracket as overall design space for the topology optimization, see Figure 13.

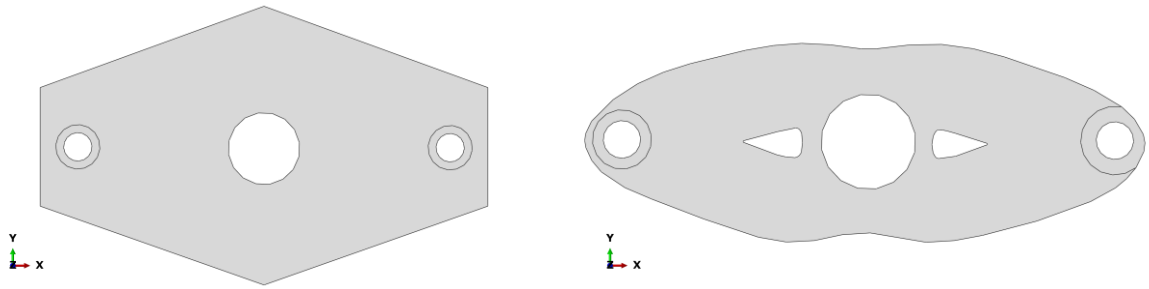

Figure 13: Topology optimization of the geometry on the left. The optimized design is shown on the right. For the topology optimization the Abaqus Tosca is used.

From the topology optimized design the optimal fibre vectors are defined using the control point method described in previous work [1]. From the result the fibre paths are defined using the in-house tool PathFinder, see Figure 14. In theory the final result can be printed using the continuous fibre technology however the Eiger software does not allow to import your own designs. Further issues could arise with very short fibre paths that currently cannot be printed.

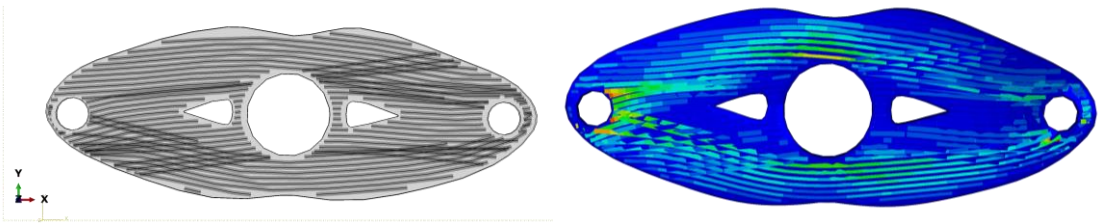

Figure 14: Optimized design with fibre steering for 3D printing. The finite element results on the right shows the independent mesh method on this design.

The design uses one layer and a thickness of one millimetre for the nylon part. The curvature around the central hole can be observed as a result of the optimization. Because of an offset in the fibre layer there is significant bending which nicely shown how the method works.

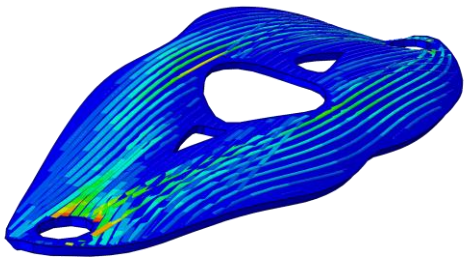

Figure 15: 3D view on the part with bending observed caused by the offset of the fibres in the nylon material

With the current state of the manufacturing this type of design cannot be printed and tested. However a comparison with the concentric designs used for the MarkForged printer can be made using this virtual test approach. This is future work that will be performed including comparisons with typical aluminium and composite aerospace components.

4 CONCLUSIONS

In this paper a novel analyses method has been proposed for 3D printed nylon parts with continuous carbon fibre reinforcement. The mechanical properties resulting from the tests performed at the NLR show that the strength and stiffness increase compared to typical 3D print plastic e.g. nylon, PLA, ABS is significant. This makes the material interesting for use in low or medium loaded part in an aircraft. For example bracket in the interior or seat-frames which are currently made from aluminium. In theory a weight gain can be achieved with the high specific stiffness and strength of the continuous fibre reinforced nylon although more research is needed. The reinforcement is in one layer and the strength perpendicular to this layer is very low, the strength of nylon. Hence typical applications are where the load is transferred in a 2D plane. Furthermore quality issues are observed with the current process such as voids and large delaminations.

The analyses method presented using an independent mesh for the carbon fibre yarns and for the nylon material is promising. It allows for efficient evaluation of the designs that are generated in e.g. the Eiger software of the MarkForged printer. The performance of the design can be evaluated and if needed adjusted with e.g. more concentric carbon fibre rings in the part. Ultimately the method can be used to evaluate designs that currently cannot be manufactured using the current MarkForged 3D printer including fibre steering aspects to further improve the performance. With the presented approach, 3D printing with continuous carbon fibres is moving from the trial and error approach currently used to right first time designs.

ACKNOWLEDGEMENTS

The support of Floyd Shackelford of Shackman's Hub is kindly acknowledged.

REFERENCES

[1] W.M. van den Brink, W.J. Vankan, R. Maas, Buckling-optimized variable stiffness laminates for a composite fuselage window section, ICAS 2012 conference, Brisbane, Australia

[2] W.M. van den Brink, R. Bruins, P. Lantermans and C. Groenendijk, Fibre steered skin design of composite thermoplastic horizontal stabilizer torsion box, 5th Aircraft Structural Design Conference, Manchester, 4 - 6 October 2016

[3] W.M. van den Brink, G. van de Vrie, and M. Nawijn, Modelling and simulation of damage in woven fabric composites on meso-macro level using the independent mesh method, International Journal of Materials Engineering Innovation 2013 4:2, 84-100

[4] W. Zeng, Y. Liu , J. Deng, Y. Guo, K. Jiang, P. Wang, Z. Yu, and Y. Shen, "Laser Intensity Effect on Mechanical Properties of Wood-Plastic Composite Parts Fabricated by Selective Laser Sintering," *Journal of Thermoplastic Composite Materials,* vol. 26 (1), pp. 125–36, 2001

[5] S. Huang, P. Liu, A. Mokasdar, and L. Hou, "Additive manufacturing and its societal impact: a literature review," *Int J AdvManf Technol*, vol. 67, pp. 1191 – 1203, 2013

[6] A. Busachi, J. Erkoyuncu, P. Colegrove, R. Drake, C. Watts, F. Martina, "Defining Next-Generation Additive Manufacturing Applications for the Ministry of Defence (MoD)", *Procedia CIRP*, vol. 55, pp. 302-307, 2016.

[7] B. Berman, "3-D printing: The new industrial revolution," *Business Horizons*, vol. 55, pp. 155–162, 2012.

[8] F. Rengier, A. Mehndiratta, and H. von Tengg-Kobligk, "3D printing based on imaging data: review of medical applications," *Int J CARS*, vol. 5, pp. 335–341, 2010.

[9] Hague, R, I Campbell, and P Dickens. 2003. "Implications on Design of Rapid Manufacturing. " *Proceedings of the I Mech E Part C Journal of Mechanical Engineering Science* 217 (1): 25 –30.

[10] Hague, Richard, Saeed Mansour, and Naguib Saleh. 2003. "Design Opportunities with Rapid Manufacturing." *Assembly Automation* 23 (4): 346–56.

[11] I. D. Harris, "Additive manufacturing: A transformational advanced manufacturing technology," *ADVANCED MATERIALS & PROCESSES*, vol. 170, pp. 25–29,may 2012.

[12] C.S. Lee, S.G. Kim, H.J. Kim, and S.H. Ahn, "Measurement of anisotropic compressive strength of rapid prototyping parts", *Journal of Materials Processing Technology*, vol. 187-188, pp. 627-630, 2007.

[13] S. Kumar and J.-P. Kruth, "Composites by rapid prototyping technology," *Materials and Design*, vol. 31, pp. 850–856, 2010.

[14] F. Ning, W. Cong, Y. Hu and H. Wang, "Additive manufacturing of carbon fiber-reinforced plastic composites using fused deposition modeling: Effects of process parameters on tensile properties", *Journal of composite materials*, vol. 51, pp. 451-462, 2016.

[15] C. Hsueh, "Young's modulus of unidirectional discontinuous-fibre composites," *Composites Science and Technology*, vol. 60, pp. 2671 – 2680, 2000.

[16] H. Tekinalp, V. Kunc, G. Velez-Garcia, C. Duty, L. Love, A. Naskar, C. Blue, and S. Ozcan,"Highly oriented carbon fiber-polymer composites via additive manufacturing," *Composites Science and Technology*, vol. 105, pp. 144–150, 2014.

[17] M. Namiki, M. Ueda, A. Todoroki, Y. Hirano, and R.Matsuzaki, "3D Printing of Continuous Fiber Reinforced Plastic," in *Society of the Advancement of Material and Process Engineering (Seattle)*, p. 6, SAMPE, jun. 2014, jun 2014.

[18] F. van der Klift, Y. Koga, A. Todoroki, M. Ueda, Y. Hirano, R. Matsuzaki, 3D Printing of Continuous Carbon Fibre Reinforced Thermo-Plastic (CFRTP) Tensile Test Specimens, Open Journal of Composite Materials, 2016, 6, 18-27

[19] R.Matsuzaki, M. Ueda,M.Namiki, T.-K. Jeong, H. Asahara, K.Horiguchi, T.Nakamura, A. Todoroki, and Y. Hirano, "Three-dimensional printing of continuous-fiber composites by in-nozzle impregnation," *Scientific Reports*, vol. 6, 2016.

[20] L. Love, V. Kunc, O. Rios, C. Duty, A. Elliott, B. Post, R. Smith, and C. Blue, "The importance of carbon fiber to polymer additive manufacturing", Journal of Materials Research, vol. 29(17), 1893-1898, 2014.

[21] ASTM D3039–14, "Standard test method for tensile properties of polymer matrix composite materials," 2014. [Online; accessed 24-November-2016].

[22] ASTM D790–03, "Standard test method for tensile properties of plastics," 2003. [Online; accessed 24-November-2016].

[23] European Association of Aerospace Industries, "Din en2850," 1997.